Title: Technology of production of Syrian lustre (11th to 13th century)

Authors: T. Pradell, R. Fernandes, G. Molina, A.D. Smith, J. Molera, A. Climent-Font, M.S. Tite

PII: S0955-2219(18)30073-6
DOI: https://doi.org/10.1016/j.jeurceramsoc.2018.01.046
Reference: JECS 11714

To appear in: *Journal of the European Ceramic Society*

Received date: 8-9-2017
Revised date: 28-1-2018
Accepted date: 30-1-2018

Please cite this article as: Pradell T, Fernandes R, Molina G, Smith AD, Molera J, Climent-Font A, Tite MS, Technology of production of Syrian lustre (11th to 13th century), *Journal of The European Ceramic Society* (2010), https://doi.org/10.1016/j.jeurceramsoc.2018.01.046

Technology of production of Syrian lustre (11th to 13th century)

T. Pradell[1], R. Fernandes[2], G. Molina[1], A.D. Smith[3], J. Molera[4], A. Climent-Font[5] and M.S. Tite[6]

[1]Physics Department, Barcelona Research Center in Multiscale Science and Engineering, Universitat Politècnica de Catalunya, Campus Baix Llobregat. c) EsteveTerradas 8, 08860 Castelldefels, Spain

[2]Faculdade de Ciências e Tecnologia, Vicarte, Universidade Nova de Lisboa, 2829-516 Monte de Caparica, Portugal

[3]Dalton Cumbrian Facility. University of Manchester, Westlakes Science & Technology Park, Moor Row, Cumbria CA24 3HA, UK

[4]MECAMAT, Universitat de Vic - Universitat Central de Catalunya, Campus Torre dels Frares, c) de la Laura 13, 08500 Vic, Spain

[5]Centro de Micro-Análisis de Materiales and Departamento de Física Aplicada, C-XII, Universidad Autónoma de Madrid, Campus de Cantoblanco, 28049 Madrid, Spain

[6]Research Laboratory for Archaeology and the History of Art, Oxford University, Dyson Perrins Building, South Parks Road, Oxford OX13QY, UK

Abstract

Lustre is a decoration consisting of a surface layer of silver and copper metal nanoparticles, a few hundreds of nanometres thick and incorporated into the glaze. It shows a colourful metallic and iridescent appearance which makes use of the quantum confined optical response of the metallic nanoparticles. Three apparently unrelated lustre decorations, yellow-orange golden (*Tell Minis*), a dark brown-reddish with iridescences (*Raqqa*) and yellow-brown golden (*Damascus*) were produced in the same area in successive periods over tin and lead-free glazes which is known to require specific strategies to obtain a metallic shiny lustre. The composition and nanostructure of the lustre layers are analysed and the materials and specific firing conditions followed in their production determined. The optical properties of the lustre layers have been analysed in terms of the nanostructure obtained and correlated to the specific processing conditions.

Keywords: Silver nanoparticles; Copper nanoparticles; Optical properties; SPR

Introduction

Lustre is a glaze decoration with a colourful metallic and iridescent appearance which makes use of the quantum confined optical response of metallic nanoparticles (Surface Plasmon Resonance, SPR). Lustre is a micrometric layer, from few hundreds of nanometres up to

several microns thick, made of metallic silver and/or copper nanoparticles (≈ 2 nm to 100 nm) beneath the glaze surface[1-5].

Lustre production starts with ion exchange between metal ions (Ag^+ and Cu^+) from an initial mixture applied on the glaze surface, which is fully removed after firing, and alkali ions (Na^+ and K^+) from the glaze; then diffusion of the metal ions inside the glaze surface, reduction of the metal ions to the metallic state (Ag^+ to Ag^0 and Cu^+ to Cu^0) and finally, nucleation and growth of metallic nanoparticles[6,7]. The reduction of the metal ions to the metallic state is obtained either applying an external reducing gas or adding reducing agents to the glaze (Sn^{2+}, Fe^{2+})[6]. Lustre must be fired at a temperature above the glass transition temperature to boost ionic diffusivity of the alkali ions, and below the softening temperature to avoid the lustre mixture sticking to the glaze. Specific materials and firing procedures give rise to differences in the lustre nanostructure and consequently to differences in the colour (green, yellow, amber, red, brown, white), and metallic (golden, coppery, silvery) or iridescent (bluish, purplish) shine. The yellow-greenish and red colours obtained are due to the dominant dipolar contribution to the SPR absorbance cross section of silver nanoparticles (≤ 30 nm) and copper nanoparticles (≤ 50 nm), respectively, but also to the relative amount and oxidation state of silver and copper in the layer[7-9]. For larger nanoparticles, higher SPR multipolar contributions become more important and are responsible for the splitting and red shift of the silver absorption peak and also for the increase in the scattering contribution[10,11], changing the colour of silver lustres from yellow-greenish to orange then brown and creating blue-purplish iridescences[7,9,12].

Nevertheless, the most distinctive characteristic of lustre is the metallic like shine; golden[9,12] or coppery[13] from silver and copper nanoparticles respectively. Similarly to what happens in photonic materials[14], the optical response of an ensemble of particles cannot be attributed to the scattering by individual particles but rather from the collective effect[15] which produces intense colours and strong reflectance. Generally speaking, a higher concentration of metallic nanoparticles and/or of their size increase the scattering effect[5-9]**. This** may be obtained by reducing the diffusivity of the ions in the glaze, and can be achieved by simply adding large divalent cations[16,17] into the glaze such as barium or lead[7] and introducing a stronger reducing atmosphere.

Although all this may suggest a product of modern nano-technology, the fact is that the first lustre was produced at least 1250 years ago. The complexity of lustre technology suggests a direct transmission of knowledge between production centres as copying is improbable. Consequently, it is commonly accepted that the main mechanism of geographical expansion of lustre technology occurred by the migration of artisans to other production centres[18,19,20].

Previous studies demonstrated that each lustre production has distinctive characteristics: chemistry (silver/copper content and oxidation state), nanostructure (size and concentration of particles) and layer thickness[2-9,12-14,20,21]. Differences in all cases are related to a combination of variations in the production process and materials used. In particular, the addition of PbO to the alkaline glaze increases the probability of obtaining a lustrous layer; an increase from nearly 0 up to 30 wt% in the PbO content is observed from Abbasid to Fatimid lustres[9]. The low lead content of some of the earliest polychrome Abbasid productions prevented them from attaining a metallic lustrous layer[7]. A high firing temperature, stronger reducing atmosphere

and the application of several lustre pigments with successive firings[8] helped to increase the size and concentration of nanoparticles in the lustre layers, were thus required. Subsequent productions used mixed lead-alkali glazes with the exception of some Syrian and Iranian productions[20,22]; in particular, the Syrian lustreware productions which are the subject of this work.

During the 11th century Syria was under the Fatimid rule until the Seljuks took control (c. 1084–1086. Later Saladin (c. 1175–1185) conquered Syria and established the Ayyubid dynasty until defeated by the Mamluks (1260-1400). Three lustreware productions directly related to the Seljuk, Ayyubid and Mamluk periods exist: *Tell Minis* (late 11th- first half of the 12th century AD), *Raqqa* (second half of the 12th-first half of the 13th century AD) and *Damascus* (second half of the 13th century AD)[18,19]. The names are given after the geographical areas where main workshops (*Raqqa* and *Damascus*) or some fine objects (*Tell Minis*) have been found. The three productions are characterised by the use of stonepaste bodies (a synthetic ceramic paste made of sand, clay and glass frit), tin-free glazes and apparently unconnected lustre decorations. *Tell Minis* ware has distinctive fine compact bodies, a transparent mixed lead-alkaline glaze and a range of greenish-yellow to orange golden lustre (**Figure 1a**)[23,26]; *Raqqa* ware is coarser and more porous, has an alkaline glaze and a dark brown-reddish lustre with iridescences (**Figure 1b**)[22,24-26]. Finally, *Damascus* ware often shows more rounded sand grains, has a cobalt tinged either alkaline or mixed lead-alkaline glaze and a yellow-brown golden lustre (**Figure 1c**)[23,24,26].

Consequently, the study of Syrian lustreware is of particular interest not only because of the variety of apparently unrelated lustre decorations produced in the same area in successive periods, but also because of the use of tin-free and, at Raqqa, lead-free glazes which require specific strategies to obtain a metallic shiny lustre. Analysis of the composition and nanostructure of the lustre layers provides information about the technology of production. The differences observed between productions will be discussed in terms of the processes followed and of the optical properties obtained.

The chemistry, oxidation state and nanostructure of the lustre layers are obtained by combination of microanalytical techniques. Imaging of the lustre layers is obtained by Scanning Electron Microscopy (SEM) of Focused Ion Beam (FIB) cut and polished lustre cross sections; the crystalline compounds are identified by micro X-Ray Diffraction (μ-XRD); analysis of the lustre layers is either by an Energy-Dispersive X-ray Spectroscope attached to the SEM (EDS) or by Rutherford Backscattering Spectroscopy (RBS); the oxidation state of copper in the lustre layers is by X-ray Absorption Near Edge Structure spectroscopy (XANES) and the identification of the SPR from metallic nanoparticles by Ultraviolet and Visible spectroscopy (UV-Vis).

Materials and methods

Two *Tell Minis* (EA2217r and p8834/p8836)[27], five *Raqqa* (p9404, p620, p9403, p18777 and p18779) [28], and one *Damascus* (p8839)[27] shards were obtained from the Ashmolean Museum (Oxford), and three *Damascus* (c1293, c1295 and c1288) shards from the Victoria and Albert Museum. Pictures of all the samples analysed are given in the **tables S-I, S-II** and **S-III** and **S-IV**

in the supplementary material for the three lustre productions. Pictures of representative examples of the three types of decorations are shown in **Figure 1**.

A crossbeam workstation (Zeiss Neon 40) equipped with SEM (Shottky FE) and Ga^+ FIB columns, was used to prepare cross sections of the lustre layers[29]. First, the sample surface was coated with a thin protective Pt layer (1µm) by ion-beam-assisted deposition; then the cross section was cut and polished and a thin layer of Pt deposited to enhance conductivity. SEM images of the polished cross sections of the lustre layers were obtained at 5 kV (some at 2 kV). In some cases chemical line maps of cross sections of the lustre layers were also obtained. The compositions of ceramic pastes and glazes were obtained from polished cross sections by SEM-EDS (INCAPentaFETx3 detector, 30mm^2, ATW2 window) operated at 20kV, with 120s measuring times, on representative areas of paste (3 mm x 2 mm) and glaze (~200 µm x 200 µm), calibrated using mineral and glass standards respectively. The data are an average of at least 2 measurements. Optical microscope and SEM-BSE images of ceramic and glaze cross sections of some of the sherds are shown elsewhere[22].

RBS measurements were performed using a 5 MV tandem accelerator[30]. A 3070 keV energy He-beam with square-section (1 mm in diagonal) was used, thus taking advantage of the elastic resonance $^{16}O(\alpha,\alpha)^{16}O$ occurring at this energy and increasing the sensitivity to oxygen concentration by a factor of 23[31]. The samples were kept in vacuum. A careful quantification was performed by employing the simulation code SIMNRA[32]. RBS data was fitted starting from the average chemical compositions obtained from the microprobe analysis of the layers and following a procedure described elsewhere[8,9,12,13]. To determine the chemical profiles of the lustre cross sections, a sequence of layers with varying silver and/or copper content was modelled. The thickness of each layer is given in units of areal densities, which can be converted into absolute thicknesses provided that the mean density of the layer is known. The mean density of the lustre layer was estimated by linear interpolation from the metal nanoparticle and glaze fractions taking 10.49 g/cm^3 for metallic silver, 8.89 g/cm^3 for metallic copper and, for the glaze, the density calculated from the RBS fittings after Fluegel[33].

Cu K-α edge EXAFS fluorescence spectra for lustre layers p620f, c1293 and c1295r were acquired using a SDD single channel fluorescence detector at beamline CLAESS (BL22) at the Alba synchrotron. X-ray absorption Near Edge (XANES) data was collected for the lustre layers on EA2217, p620, p8833, p8834/36 and p8839 samples. In all the cases a 100x200 µm^2 area was measured. Reference Cu foil and pellets of cuprite (Cu_2O) and tenorite (CuO) powders were measured in transmission mode. Data analysis was conducted using the Demeter (Athena for XANES and Artemis for EXAFS) suite of programmes[34].

µ-XRD of cross sections of the ceramic bodies, glazes and lustre decorations were performed in transmission geometry at beamline MSPD (BL04) at the Alba Synchrotron Light Facility using 0.4243 Å wavelength and a CCD camera detector (Rayonix SX165, Rayonix, L.L.C., Evanston, IL).

UV-Vis diffuse reflectance (R) measurements were performed directly on the surface of the samples using a double beam UV-Vis spectrophotometer (Shimadzu 2700) equipped with ISR 3100 Ulbricht integrating sphere. The spot size was a slit of 5 mm x 1 mm, and measurements were made between 200 nm and 800 nm at 1 nm resolution. A D65 standard illumination source was used and barium sulphate provided a white standard.

Cu and Ag chemical cross section profiles were determined either from the RBS fitted data or from SEM-EDS line imaging. Images and cross section profiles from all the samples studied are shown in the complementary material **Tables S-I, S-II** and **S-III** and **S-IV** for the three lustre productions.

Results

Analysis of the ceramic bodies is shown in **Figure 2** and detailed data is given in the supplementary material **Table S-V**. Analysis of the glazes is given in **Table I**. All the ceramic bodies are *stonepastes* with one exception, sample p8839 of the Damascus wares, which is *earthenware*. The *stonepastes* are made of sand, clay and a glass frit, and looking at the analysis we can find differences in the raw materials used to produce them.

The chemical composition of the bodies can be compared to those published in the literature in **Figure 2**[22-24,26,35]. Three sets of published data are used: *Raqqa* lustreware from a collection of the Metropolitan Museum (MET)[25,36]; the ceramics found in the excavations of Qal'at Ja'bar[21] dated between late 11th or early 12th century AD[35] and those found in several Northern Syrian sites dated between the 8th and 14th century[24]. Two main types of stonepastes[23,24,35] are described in the literature; the first type which includes the *Tell Minis* wares is characterised by high Aluminium with low Calcium and Magnesium content, compared to the second which includes the *Raqqa* type wares.

Among the *Raqqa* wares from the MET and the Northern Syrian sites some *earthenwares* (iron rich calcareous clays) were also found[24,25,36]. The good linear correlation between Al_2O_3 and FeO found[25,36] between the *stonepastes* and the *earthenwares* (**Figure 2a**) demonstrated that the same clay used to produce the *earthenwares* was added in variable amounts to the quartz sand to produce the *stonepastes*. Moreover, the *Tell Minis* and *Raqqa stonepastes* from this study and also from the Qal'at Ja'bar[23,35] also show a good linear correlation between Al_2O_3 and FeO with the *earthenware* found in this study, p8839, **Figure 2a**. Moreover, looking at the correlation shown in **Figure 2b**, the Calcium and Magnesium were partly incorporated in the *stonepastes* with the clay and partly added with the glass frit. Finally, the Sodium content (**Figure 2c**) cannot be related to the clay added in any of the cases, but is attributed to the glass frit[23-26]. This demonstrates that at least two different clays were used to produce the Syrian *stonepastes*.

Among the *Damascus* wares, two *stonepastes* are also identified **(Figure 2**). *Damascus I* (p8039 and c1293) with high Aluminium and low Iron, Calcium and Magnesium. These are similar to the *Tell Minis* lustrewares, while *Damascus II* (c1288 and c1295) have higher Calcium and Magnesium content, in better agreement with the *Raqqa* wares.

In summary, two clays were used; one with low Iron, Calcium and Magnesium and high Sodium content used in the production of *Tell* Minis, some *Raqqa*, *Damascus type I* and also other luxurious wares[23,36], and the second with high Iron, Magnesium and Calcium and lower Sodium used in the production of some *Raqqa*[25,36] and also *Damascus II*. This demonstrates that both types of *stonepastes* continued being used later in the second half of the 13th century.

μ-XRD of the pastes shows the presence of Quartz (SiO_2), Cristobalite (a high temperature polymorph of quartz, (SiO_2)), Nepheline ($NaAlSiO_4$) and Diopside ($CaMgSi_2O_6$). Cristobalite, Nepheline and Diopside are formed by reaction of the clay and glass frit with quartz grains at a temperature between 950°C-1000°C. Calcite is also present in the *Raqqa* and *Damascus* wares. Considering that calcium is added to the *stonepastes* through the glass frit or incorporated with the clay, this Calcite can only be either recrystallized from original large Calcite grains after firing or the result from contamination during burial. Given the large porosity shown by some of the wares, in particular Raqqa wares the latter cannot be withdrawn[23].

The three lustreware productions also show distinct glazes. Their chemical composition is shown in **Table I**[23]; *Tell Minis* glazes are mixed soda rich alkaline-lead with about 15-20% PbO while *Raqqa* glazes are soda rich alkaline. Moreover, *Damascus I* glazes with bodies matching those of *Tell Minis* are also mixed alkaline-lead with about 20% PbO while *Damascus II* glazes with bodies matching those of *Raqqa* are soda-rich alkaline but contain more Calcium, Magnesium and Potassium. The blue colour of the *Damascus* glazes is due to the addition of Co^{2+} and Fe^{2+} (an iron rich cobalt sulphide) and also some Cu^{2+} and Zn^{2+} (probably added as a copper scrap). Cristobalite crystallites are found in the *Damascus* glazes.

SEM images of polished cross sections of the lustre layers and the corresponding Cu and Ag profiles from characteristic *Tell Minis*, *Raqqa* and *Damascus I* and *II* lustres are shown in **Figure 3**, **4, 5** and **6** respectively. All the samples studied are shown in the complementary material **Tables S-I, S-II**, **S-III** and **S-IV**. The Cu and Ag elemental compositions across the lustre layer sections are obtained from fitting of the RBS spectra, or from SEM-EDS line scans for those lustre layers thicker than the RBS data can probe. The data shows that the lustre layer compositions and nanostructures are very characteristic and distinctive for each production.

The average Cu and Ag content (wt%), the maximum concentration (at%) and depth (μm) at which the maximum content of copper and silver is found, as well as the thickness (μm layer) of the lustre layer calculated either from the RBS fitted spectra or SEM-EDS line scans are shown in **Table II**.

The nature of the nanoparticles is determined by μ-XRD and UV-Vis spectroscopy (**Figure 7**). Metal silver and cuprite nanoparticles are found in the *Tell Minis* and *Damascus* lustres while only copper metal nanoparticles of a very small size (large XRD peaks) are found in the *Raqqa* lustres.

Silver is always in the metallic state in contrast to copper, thus the oxidation state of copper has been determined by X-ray spectroscopy. The XANES data contains features which can be compared to those in the model compound spectra (metallic copper, Cu^o; cuprite, Cu_2O for Cu^+ and tenorite, CuO for Cu^{2+}). In particular the position of the absorption edge shifts characteristically with oxidation state as shown in **Figure 8** (8982.3 eV for Cu^o, 8983.8 eV for Cu^+ and 8986.9 eV for Cu^{2+}). We find that for the *Tell Minis* and *Damascus* samples a high degree of copper oxide with an edge position in the region of 8982.8 – 8983.2 eV, along with a strong resonance at 8984.3 eV. Both of which match features seen in cuprite (Cu^+). The main peak is at 8997 eV, which is a little below the peak seen in cuprite. This small shift down in energy is explained by a small contribution of copper metal in the lustre layers with a lower energy peak at 8996 eV. This suggests an additional contribution of copper metal of between

22% and 30%. The key indicator in the XANES supporting cuprite, and hence Cu^{+}, rather than Cu^{2+} oxide lies in the position of the absorption edge which lies in the region closer to the edge position for Cu^{+} (8983.8 eV) than Cu^{2+} (8986.9 eV). The *Raqqa* sample is rather different, with a much higher metal contribution of 64%. The metal component is evidenced by the characteristic double peaks at 8997 and 9006 eV and a shift of the absorption edge to slightly lower energy as expected for Cu^{0}. A summary of the chemical species is also given in **Table II** and the full results of least squares fitting of model compound data to the experimental data are given in **Table S-VI**.

The full EXAFS data were also taken from two of the *Damascus* samples (c1293 and c1295) and one from *Raqqa* (p620r), **Figure 9** and **Table III** (full results of fitting of model compound data to the experiment are given in **Table S-VII**) These confirmed that the principle oxide content in the *Damascus* lustre is from a cuprite like structure (Cu-O first shell bond distance closer to the 1.85 Å of cuprite, rather than the 1.96 Å of tenorite), and also the dominant copper metal contribution in the *Raqqa* lustre. However, the amplitude of the EXAFS oscillations in sample c1293 was not very high, making it difficult to fit more than the first (Cu-O) shell, suggesting a lack of any longer range order which would be consistent with partially reduced oxide dissolved in the glaze. The incident X-rays used in these X-ray absorption spectroscopy measurements (XAS) will probe to a depth of at least 100 micron, so will combine data from a depth greater than the lustre layer in many cases. This is particularly important in those lustres obtained on glazes containing copper, either as a decorative motif like *Tell Minis*, or in the blue glaze itself like *Damascus I*.

Tell Minis lustres are copper rich, above 70% Cu/(Ag+Cu) (**Table II**), with the copper being mainly oxidised (78%) as Cu^{+} (**Table II**). Metallic silver and cuprite nanoparticles are identified with a very low amount of metallic copper nanoparticles (**Figure 7 and 9**). The lustre layer is ≈2µm thick and contains a gradient of nanoparticles, smaller near the surface (below 20 nm) and larger (above 70 nm) inside the glaze (**Figure 3b** and **3c**). Silver appears mainly concentrated near the surface (≈200 nm) while copper appears in a broader layer with the maximum concentration at a depth below the surface of about 1 µm (**Figure 3D**). The uneven silver richer surface layer appears partly lost, indicating that the lustre layers are not well preserved.

Raqqa lustres are richer in copper, often close to 100%Cu/(Cu+Ag), and mainly constituted by very small metallic copper nanoparticles (**Figures 7** and **9,** and **Table II**). The lustre layer is ≈0.5 µm thick and contains very small nanoparticles (less than 20 nm) (**Figure 4b** and **4c**). The layer shows a peaked Cu profile with a maximum copper content at ≈200 nm (**Figure 4d**).

The *Damascus* lustre layers are copper rich (above 56% Cu/(Cu+Ag)) and the copper appears mainly oxidised (**Figure 8** and **9**, **Table III)**. Both metallic silver and cuprite nanoparticles are found (**Figures 7**). *Damascus I* layers are about ≈4-5 µm thick (**Figure 5b**) while those of *Damascus II* are thicker (≈5-10 µm) (**Figure 6b**. This is consistent with the application of a lead free glaze in *Damascus II*. The layers are typically structured with a particle-free top (≈150-250 nm thick layer) followed by ≈40 nm thick layer where the nanoparticles coalesce into larger non-spherical aggregates (**Figure 5c**) and into a continuous metallic layer (**Figure 6c**). Then there is a layer (≈2 µm and ≈5-9 µm thick for *Damascus I* and *Damascus II* respectively)

containing nanoparticles of increasing particle size (the largest particles of about 90 nm size) (**Figure 5c** and **Figure 6c**). Metallic silver and copper are concentrated in the first thin particle layer near the surface; some large metallic silver particles are also found at the end of the second particle layer while copper shows a maximum concentration between both particle layers (**Figure 5d** and **Figure 6d**). In some isolated spots the layer is thicker (up to 40 μm) formed by several sublayers of nanoparticles (≈10-15 μm) separated by particle free regions (≈3-8 μm). The lead-alkali glazes used in *Damascus II* lustreware is responsible for the development of thinner lustre layers and also of the formation of a continuous thin metallic layer near the surface.

In summary, *Tell Minis* lustre layers are single 2 μm thick and copper rich (≈70% Cu/(Cu+Ag)) although only 20% of the copper is reduced to the metallic state. They are formed mainly by metallic silver nanoparticles concentrated near the surface (<0.2μm) with cuprite and a small amount of metallic copper nanoparticles (concentrated at ≈1μm). *Raqqa* lustre layers are single and very thin (≈0.5 μm), copper rich (≈100% Cu/(Cu+Ag)) and formed only by very small metallic copper nanoparticles (<20 nm). *Damascus I and II* lustre layers are very thick (4-5 and 5-10 μm respectively), copper rich (≈60 % Cu/(Cu+Ag)). They show a multilayer structure: a first particle-free top layer (≈150 and 250 nm thick), a second ≈40 nm thick layer where the metallic silver nanoparticles coalesce into larger non-spherical aggregates for *Damascus I* and into a continuous metallic layer for *Damascus II* lustres. They have a cuprite rich intermediate thick layer (several microns thick) which ends with larger nanoparticles.

Discussion

Dissimilarities among the optical properties (colour, shine, opacity, etc.) of the three lustre productions are directly related to the differences in the chemical composition, copper speciation, nature and size of the nanoparticles, as well as to the concentration of particles and thickness of the lustre layers. In their turn, these differences depend on the composition of the lustre mixture used, glaze composition and firing conditions. The lustre precursor is fully removed after firing and consequently its composition is usually unknown[37].

Generally speaking lighter reducing conditions are required to reduce silver ions than is the case for copper ions. In fact Cu^{+} ions are able to reduce silver to the metallic state while they oxidising themselves to Cu^{2+}, which then dissolves in the glaze. Therefore, the addition of copper lustre helps the precipitation of silver nanoparticles. Small silver nanoparticles (below 20 nm) produce a green-yellowish colour as they have strong SPR absorption at about 420-430 nm, and the presence of Cu^{2+} with a broad absorption in the red will enhance this effect[7,9,12]. Applying a reducing atmosphere promotes the growth of the silver nanoparticles, reduces Cu^{2+} back into Cu^{+} and the crystallisation of cuprite nanoparticles and in the case of a strong reducing atmosphere the reduction of copper to the metallic state and precipitation of metallic copper nanoparticles. Larger metallic silver nanoparticles and cuprite nanoparticles shift the colour of the lustre layer towards yellow-orange[7,9,12]. The presence of metallic copper nanoparticles absorbing at larger wavelengths (~560 nm) shifts the lustre layers colour to brown.

Consequently, metallic silver nanoparticles may be obtained by firing under light reducing conditions, especially using mixed silver/ copper lustres, and the main presence of Cu^{+} is evidence of the use of light reducing conditions. The presence of smaller particles near the surface in *Tell Minis* in comparision to *Damascus* lustres indicates the use of lighter reducing conditions. The relative thin *Tell Minis* lustre layers (2-3 μm), compared to *Damascus* (4-10 μm), also indicates a shorter firing time (typically about 30 minutes[7]).

Copper lustres require stronger reducing conditions, and even if this is the case, copper is rarely fully reduced to the metallic state; besides, the addition of some silver will re-oxidise some of the copper into Cu^{+}. The colour is mainly red due to the SPR absorption of the metallic copper nanoparticles, varying to dark brown if metallic silver nanoparticles are also present. *Raqqa* lustre layers are thin and the copper is fully reduced to the metallic state, which indicates a very short strong reducing firing (typically about 10 minutes[7]).

The firing temperature depends basically on the composition of the glaze. The glass transition temperature (T_g) marks the transition from solid to liquid behaviour; in particular, atomic diffusivity in the glaze is boosted above T_g[38]. Consequently, lustre has to be fired at temperatures above T_g to develop, and below the glaze softening temperature to prevent the lustre pigment sticking to the glaze surface. The glass transition and softening temperatures depends on the composition of the glaze[39]; they are lower for those glazes richer in Na, K and Pb and higher for those richer in Si, Ca and Al. In particular, both *Raqqa* and *Damascus II* have soda-lime glazes for which $T_g \approx 530^{o}C$ (Littleton glass softening temperature ≈ 730°C). The substitution of calcium by lead reduces the glass transition temperature; for a typical mixed lead-soda glass of composition similar to *Tell Minis* and *Damascus I* the calculated $T_g \approx 490^{o}C$ (glass softening temperature ≈ 670°C[39,40]), about 40°C lower than those of *Raqqa* and *Damascus II* glazes.

The addition of divalent ions such as Pb in the glaze (about 20% PbO in *Tell Minis* and *Damascus I*) reduces the diffusivity of the ions[16,17] and gives rise to more concentrated lustre layers which are responsible for the metallic shine. Consequently, shiny lustre layers are more difficult to achieve on alkaline glazes. In fact, *Raqqa* lustres rarely show metallic shine, and metallic shine is not exhibited in any of the samples studied; the copper nanoparticles are very small (<20 nm) with a large surface area - the consequence of a short, strong reducing stage. In particular for metallic copper nanoparticles, the size of the particles is important in achieving the metallic effect as scattering is very small and absorption dominates the optical response for particles smaller than 40 nm.

Nevertheless, a concentrated shiny lustre layer may still be obtained using a higher temperature and stronger or longer reducing firings. A long firing will accumulate more silver and copper in the lustre layer and make it thicker. Both higher temperature and stronger reducing conditions favour the growth of metallic nanoparticles which may coalesce and form large aggregates, or even a continuous nanometric metallic layer (*Damascus II*), near the surface. The absence of metallic copper nanoparticles in the *Damascus* lustres indicates the use of higher temperatures rather than stronger reducing conditions. The use of lead-alkali glazes in *Damascus II* helps a greater accumulation of the metals and the formation of the continuous thin metallic layer.

The reflection of continuous nanometric silver metallic layers of various thicknesses over a glass substrate may be calculated using Fresnel equations and the transfer matrix method[41]. The colour coordinates of the light reflected may also be determined using the protocol accepted by the International Commission for Illumination, CIE *L*a*b** (International Colour Consortium 1976). The hue ($h^* = tan^{-1}\left({}^{b^*}/_{a^*}\right)$), relative saturation ($c^* = \sqrt{(a^*)^2 + (b^*)^2}$) and lightness (*L**) of the Reflectance are plotted as a function of the silver metallic layer thickness in **Figure 10**. Thin layers below 40 nm have a high saturation, the colour varies from yellow-reddish to yellow-greenish, and the lightness increases from 40% up to nearly 100. Increasing the thickness of the layer decreases the hue dramatically down to zero and the colour shifts again to a yellow-reddish. Layers of about 30 nm show a saturated yellow hue and high lightness, together with a golden shine effect. Thicker layers, above 50 nm thick, show already low saturation and high lightness, *i.e.* a silvery shine (**Figure 10)**. Consequently, the presence of silver aggregates (some hundreds of nm in size and some tens of nm thick), or of a thin silver metallic layer (some tens of nm thick) will increase the shine, resulting in yellow (golden shine) for thin layers (30-40 nm) and white (silvery shine) for thicker layers.

In summary, the various lustre layers are consequence of different products and firing conditions. *Tell Minis* lustre layers were produced over lead-alkali glazes and show the characteristic double layer lustre[5,6] consisting of a thin surface silver layer (<0.2 μm) and copper rich layer (≈1 μm) where copper is mainly oxidised (Cu^+ dissolved and cuprite nanoparticles). This is characteristic of a light reducing firing, at low temperature (above T_g ≈500°C) and typical firing time of about 30 minutes. The yellow-orange colour is mainly due to the presence of silver and also of cuprite nanoparticles. The golden shine which is common in this production is due to the presence of a high concentration of silver nanoparticles in the layer, although the samples studied here do not show it due to the deficient preservation of the lustre layers.

Raqqa lustre layers were obtained over alkali glazes and show a single and very thin layer (≈0.5 μm) close to the glaze surface[5] containing very small metallic copper nanoparticles (<20 nm), amorphous Cu^+, and only very small amount of silver nanoparticles if present. This is obtained using a short strong reducing firing, at low temperature (above T_g ≈ 550°C) and typical firing time of about 10 minutes. The colour is red due to the SPR absorption of Cu nanoparticles, and brown for those also containing silver nanoparticles. The size of the metallic particles is not large enough to produce the metallic shine in the samples studied and it is rarely observed in the *Raqqa* lustre production.

Damascus I and II lustre layers were obtained over lead-alkali and alkali glazes respectively. They are extremely thick, show a multi-layered structure[5] and contain mainly metallic silver and cuprite nanoparticles. The yellow to brown colour is due to the SPR absorption of silver nanoparticles and of cuprite nanoparticles. The layers have a first superficial thin layer of metallic silver nanoparticles merging into larger aggregates for *Damascus I* and into a continuous metallic layer for *Damascus II*. This 30 to 40 nm thick, more or less continuous silver metallic layer, is responsible for the golden shine. This structure results from a long high temperature firing; thicker layers produce a silvery shine in which case a long stronger reducing firing must have been used. Nevertheless the control of the process, in particular for

those obtained over alkali glazes, must have been difficult and *Damascus* lustre showing a silvery shine is not unusual.

Conclusions

The results demonstrate that both finer and coarser stonepaste bodies were being produced in Syria during the whole period from 11th century to 13th century. The former group is characterised by the use of a low FeO, CaO and MgO clay and finer ground quartz with the application of a lead-alkali glaze, and the latter group by the use of a high FeO, CaO and MgO clay and coarser ground quartz with the application of an alkaline glaze.

Associated with these two groups, three different types of lustre with clearly distinctive composition, nanostructure and methods of production were observed, the first from Tell Minis with fine stonepaste bodies and lead-alkali glazes, the second from Raqqa with coarse stonepaste bodies and alkali glazes, and the third from Damascus which includes both fine and coarse stonepaste bodies plus their corresponding glazes.

Tell Minis lustre layers were produced over lead-alkali glazes and show the characteristic double layer lustre of metallic silver and cuprite nanoparticles responsible for the yellow-orange colour. The layers were obtained with a long low-temperature light-reducing firing.

Raqqa lustre layers were obtained over alkali glazes and show a single very thin layer containing very small metallic copper nanoparticles and also a very small amount of silver nanoparticles responsible for the red and brown colour; these layers result from a short low-temperature strong-reducing firing. The size of the copper metallic particles is not large enough to produce the metallic shine and it is rarely observed in the Raqqa lustre production.

Damascus lustre layers were obtained over lead-alkali and alkali glazes respectively and show a multi-layered structure containing metallic silver and cuprite nanoparticles. The golden shine is due to the presence of a more or less continuous thin metallic silver layer (30 to 40 nm thick) characteristic of a long high-temperature firing.

Acknowledgements

The Ashmolean Museum (Oxford) and the Victoria and Albert Museum (London) are gratefully acknowledged for providing the ceramics, together with the help provided by Marion Rosser-Owen from the V&A Museum and Alessandra Cereda from the Ashmolean Museum. Professor Oliver Watson is gratefully acknowledged for his advice in the selection of the samples. Dr. Dylan T. Smith and the Metropolitan Museum of Art (New York) are also gratefully acknowledged for granting access to the data from the Raqqa ceramics. Funding is gratefully acknowledged from CICYT grant MAT2013-41127-R and MAT2016-77753R and Generalitat de Catalunya grant 2014SGR-581. The XANES and EXAFS experiments were performed at BL22 CLAESS beamline and the micro-XRD data were obtained in BL04 MSPD beamline at ALBA Synchrotron with the collaboration of ALBA staff. This study was part of the Master thesis of Raquel Fernandes, “Characterisation of lustred ceramics from Syria and Iran (13th-14th centuries)” in Faculdade de Ciências e Tecnologia, Universidade Nova de Lisboa. The authors would also like to thank Trifon Trifonov Todorov, CRNE (UPC) for his help with the FIB-SEM.

References

1. Pradell T. Lustre and Nanostructures—Ancient Technologies Revisited. *Nanoscience and Cultural Heritage:* Chapt. 1: Dillmann P, Bellot Gurlet L, Nenner I. Ed: Atlantis Press, Springer series in Physical Chemistry; 2016
2. Pérez-Arantegui J, Molera J, Larrea A, Pradell T, Vendrell M, Borgia I, Brunetti BG, Cariati F, Fermo P, Mellini M, Sgamellotti A, Viti C. Lustre pottery from the thirteenth century to the Sixteenth century: a nanostructured metallic thin metallic film. J Am Ceram Soc 2001; **84**(2): 442-6
3. Padovani S, Sada C, Mazzoldi P, Brunetti B, Borgia I, Giulivi A, Sgamellotti A., D'Acapito F, Battaglin G. Copper in glazes of Renaissance lustre pottery: nanoparticles, ions and local environment. J Appl Phys 2003; **93**(12): 10058-63
4. Colomban P. The Use of Metal Nanoparticles to Produce Yellow, Red and Iridescent Colour, from Bronze Age to Present Times in Lustre Pottery and Glass: Solid State Chemistry, Spectroscopy and Nanostructure. J Nano Research 2009; **8**:109-32
5. Sciau Ph, Mirguet C, Roucau C, Chabanne D, Schvoerer M. Double Nanoparticle Layer in a 12th Century Lustreware Decoration: Accident or Technological Mastery?. J Nano Research 2009; **8**:133-40
6. Pradell T, Molera J, Roque J, Smith AD, Crespo D, Pantos E, Vendrell M. Ionic-exchange mechanism in the formation of medieval lustre decorations. J Am Ceram Soc 2005; **88**(5): 1281-9
7. Molera J, Bayés C, Roura P, Crespo D, Pradell T. Key parameters in the production of medieval lustre colors and shines. J Am Ceram Soc 2007; **90**(7): 2245-54
8. Molina G, Tite MS, Molera J, Climent-Font A, Pradell T. Technology of production of polychrome lustre, J Eur Ceram Soc 2014; **34**: 2563–74
9. Gutierrez PC, Pradell T, Molera J, Smith AD, Climent-Font A, Tite MS. Color and Golden Shine of Silver Islamic Lustre. J Am Ceram Soc 2010; **93**(8): 2320–8
10. Kreibig U, Vollmer M. Optical Properties of metal clustre. Springer 25. Berlin, Germany: Springer Verlag; 1995
11. van de Hulst HC. Light scattering by small particles. New York, EUA: Dover Publications Inc; 1981
12. Pradell T, Pavlov RS, Gutiérrez PC, Climent-Font A, Molera J. Composition, nanostructure, and optical properties of silver and silver/copper lustres. J Appl Phys 2012; **112**: 054307(11)
13. Pradell T, Climent-Font A, Molera J, Zucchiatti A, Ynsa MD, Roura P, Crespo D. Metallic and non-metallic shine in lustre: an elastic ion backscattering study, J Appl Phys 2007; **101**(9): 103518 (8)
14. Reillon V and Bethier S. Modelization of the optical colorimetric properties of lustred ceramics. Appl. Phys A 2006; **83** 257-65
15. Farbman I, Levi O and Efrima S. Optical response of concentrated colloids of coinage metals in the near-ultraviolet, visible and infrared regions. J. Chem. Phys 1992; **96**(9) 6477-85
16. Doremus RH. *Glass Science*. New York, EUA; John Wiley & sons Inc; 1994

17. Greaves GN and Ngai KL. Reconciling ionic-transport properties with atomic structure in oxide glasses. Phys Rev B 1995; **52**(9): 6358-80
18. Caiger Smith A. *Lustre Pottery*. New York, EUA: New Amsterdam Books; 1991.
19. Watson O. *Persian lusterware*.
20. Chabanne D, Aucouturier M, Bouquillon A, Darque-Ceretti E, Makariou S, Dectot X, Faÿ-Hallé A, Miroudot, D. Ceramics with metallic lustre decoration. A detailed study of Islamic productions from the 9th century until the Renaissance. Matériaux & Techniques 2012; **100**: 47–68.
21. Padeletti G, Fermo P, Bouquillon A, Aucouturier M, Barbe F. A new light on a first example of lustred majolica in Italy. Appl. Phys. A 2010; **100:** 747–761
22. Pradell T, Molera J, Smith AD, Tite MS. Early Islamic luster from Egypt, Syria and Iran (10th to 13th century AD). Journal of Archaeological Science 2008; **35**: 2649–2662
23. Franchi R, Tonghini C, Paloschi F, Soldi M. 1995. Mediaeval Syrian fritware: materials and manufacturing technique. *The Ceramics Cultural Heritage* Vincenzini P Ed. Faenza, Italy: Editorial Techna srl; 1995: 197–205.
24. Pérez-Arantegui J, Querré G, Kaczmarczyk A, Bernus-Taylor M. Chemical characterization of Islamic glazed ceramics from Northern Syria by particle induced x-ray emission (PIXE). *The Ceramics Cultural Heritage* Vincenzini P Ed. Faenza, Italy: Editorial Techna srl; 1995: 475–482.
25. Smith DT. Appendix 2: Compositional analysis of early-thirteen-century ceramics from Raqqa and related sites. *Raqqa Revisited. Ceramics of Ayyubid Syria* Jenkins-Madina M Ed. New York, EUA: The Metropolitan Museum of Art; 2006
26. Pradell T, Molera J, Molina G, Tite MS. Analysis of Syrian lustre pottery (12th–14th centuries AD). Appl Clay Sci 2013; **82:** 106-112
27. Porter V, *Medieval Syrian Pottery (RaqqaWare)*. Oxford, UK: Ashmolean Museum publications; 1981
28. Porter V, Watson O. Part II: Tell Minis' wares. Syrian and Iran, three studies in medieval ceramics. Oxford Studies in Islamic Art IV. Oxford, UK: Oxford University Press; 1987: 175–248.
29. Sciau P, Salles P, Roucau C, Mehta A, Benassayag G. Applications of focused ion beam for preparation of specimens of ancient ceramic for electron microscopy and synchrotron X-ray studies. Micron 2009; **40**(5-6): 597-604
30. Climent-Font A, Pászti F, García G, Fernández-Jiménez MT, Agulló F. First measurements with the Madrid 5 MV tandem accelerator. Nucl Instrum Methods Phys Res B 2004; 219-220: 400-4.
31. Cheng HS, Shen H, Tang J, Yang F. Cross sections for 170 backscattering of 4He from oxygen in the energy range of 2.0–9.0 MeV. Nucl Instrum Methods Phys Res B 1993; **83**(4): 449–53
32. Mayer M. SIMNRA user's guide; 1997 (IPP 9/113 1997): http://www.rzg.mpg.de/
33. Fluegel A. Global model for calculating room-temperature glass density from the composition. J Am Ceram Soc 2007; **90(8)**:2622–5.
34. Ravel B and Newville M. ATHENA, ARTEMIS, HEPHAESTUS: data analysis for X-ray absorption spectroscopy using IFEFFIT. J. Synchrotron Rad. 2005; **12**: 537–541.

35. Tonghini C. Qal'at Ja'bar pottery: a study of a Syrian fortified site of the late 11th-14th centuries. Oxford, UK: British Academy Monographs in Archaeology. Oxford University Press; 1999
36. Jenkins-Madina M. *Raqqa Revisited. Ceramics of Ayyubid Syria*. New York, EUA: The Metropolitan Museum of Art; 2006
37. Pradell T, Molina G, Molera J, Tite MS. Composition of the lustre pigment used in the production of 13th century AD Raqqa lustreware from Syria. Archaeometry 2016; **58(6):** 979-986
38. Bartsch A, Rätzke K, Meyer A, Faupel F. Dynamic Arrest in Multicomponent Glass-Forming Alloys. Phys Rev Lett 2010; **104**: 195901 1-4
39. Seward III T.P. and Vascott T. High temperature glass melt property database for process modelling. Westerville, Ohio, EUA: The American Ceramic Society; 2005
40. Flugel, A. Glass viscosity calculation based on a global statistical modelling approach. Eur. J. Glass Sci. Technol. A 2007; **48(1):** 13–30
41. Johnson PB, Christy RW. Optical constants of noble metals. Phys Rev B 1975; **6** (12): 4370–9

Figure captions

Figure 1. Pictures of characteristic *Tell Minis*, *Raqqa* and *Damascus* lustre decorations.

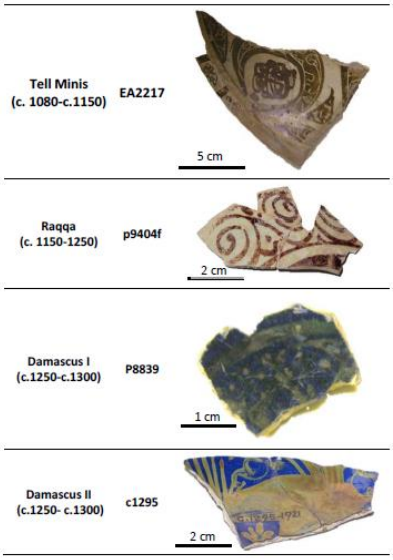

Figure 2. Chemical plots of the stonepaste bodies showing correlations between (a) FeO, (b) CaO+MgO and (c) Na_2O versus Al_2O_3 for *Tell Minis* (purple dots), *Raqqa* (dark blue dots) and *Damascus* (green dots). The plot includes also the *Raqqa* lustreware from the Metropolitan Museum, NY[25] (black dots) and all the data obtained from the samples excavated in Qal'at Ja'bar[23]; FW1 corresponds to the *Tell Minis* and other luxury wares (magenta dots) and FW2 to *Raqqa* type lustre and polychrome wares (cyan dots).

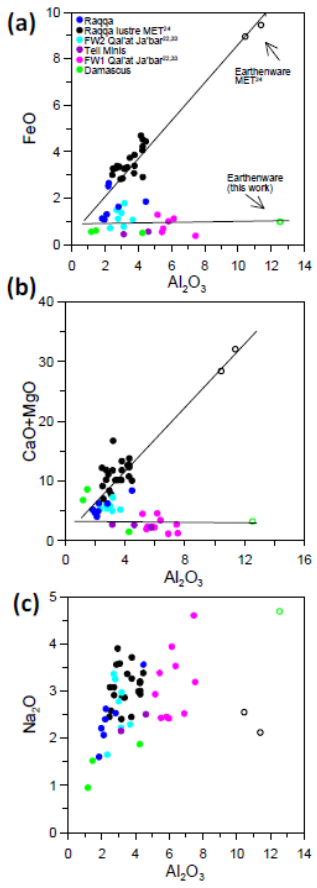

Figure 3. a) Typical *Tell Minis* lustre (p8034/36). b) Lustre cross section obtained by FIB cutting and polishing and c) magnification of the lustre cross section. d) Cu and Ag cross section profiles obtained by RBS.

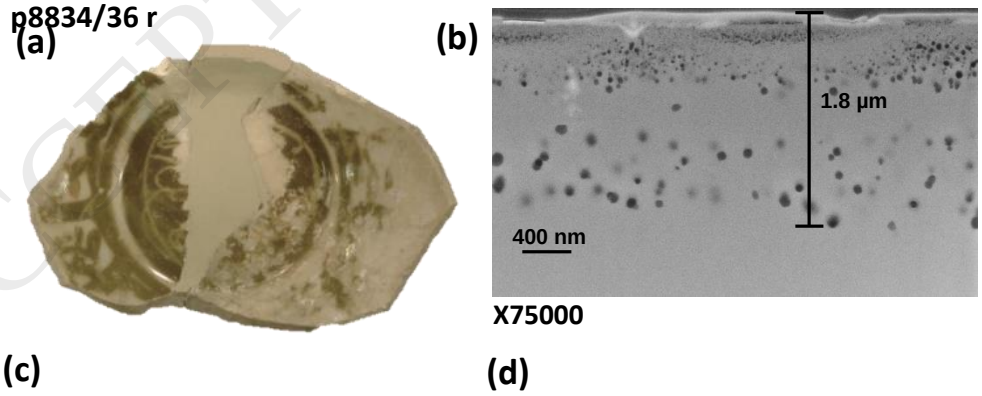

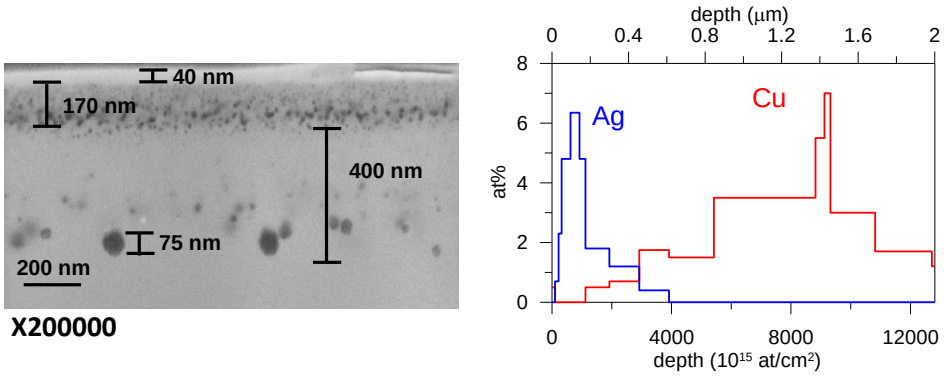

Figure 4. a) Typical *Raqqa* lustre (p18777r). b) Lustre cross section obtained by FIB cutting and polishing and c) magnification of the lustre cross section. d) Cu and Ag cross section profiles obtained by RBS.

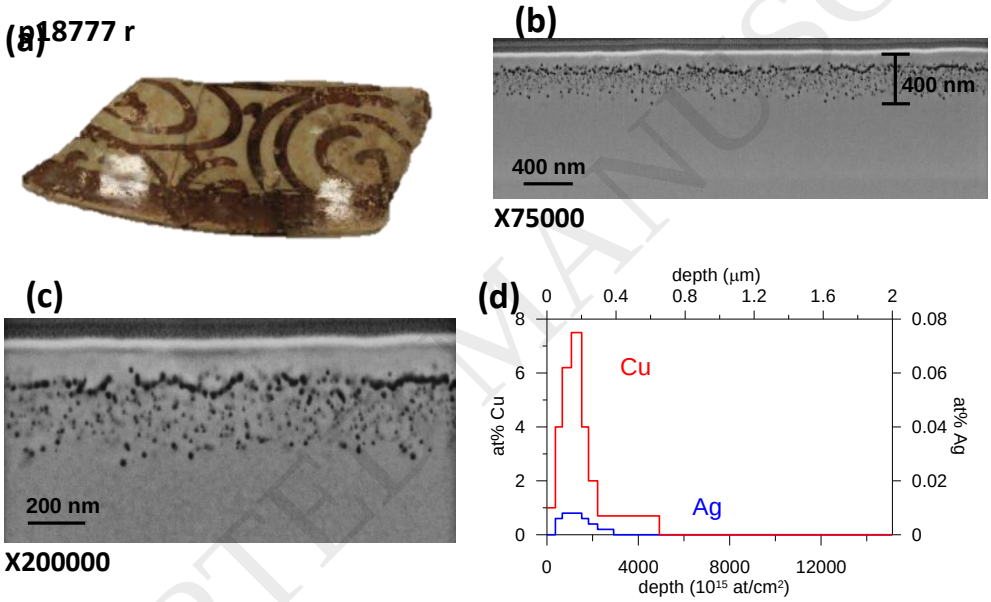

Figure 5. a) Typical *Damascus I* lustre (c1293). b) Lustre cross section obtained by FIB cutting and polishing and c) magnification of the lustre cross section. d) Cu and Ag cross section profiles obtained by SEM-EDS line scan.

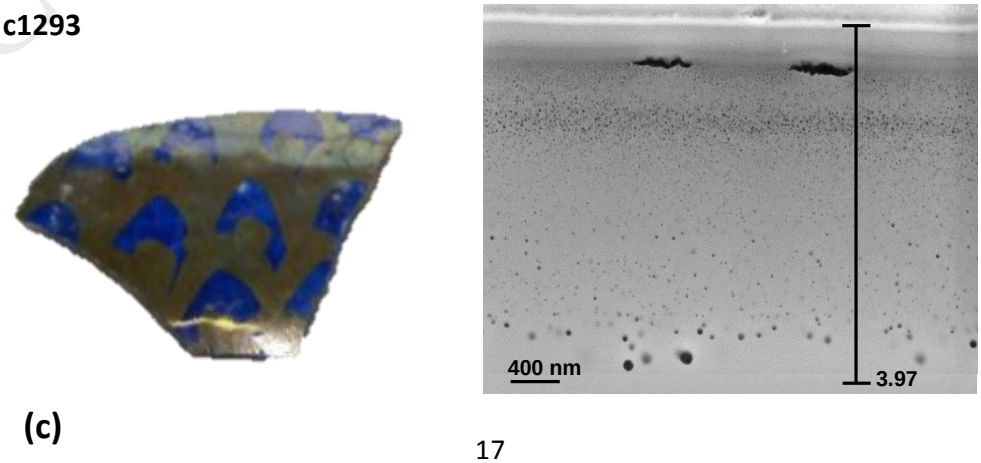

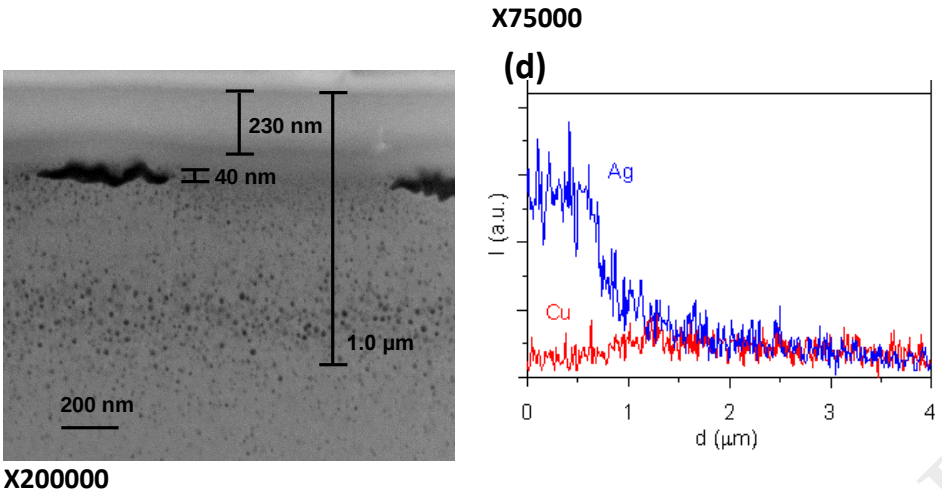

Figure 6. s) Typical *Damascus II* lustre (c1288). b) Lustre cross section obtained by FIB cutting and polishing and c) magnification of the lustre cross section. d) Cu and Ag cross section profiles obtained by SEM-EDS line scan.

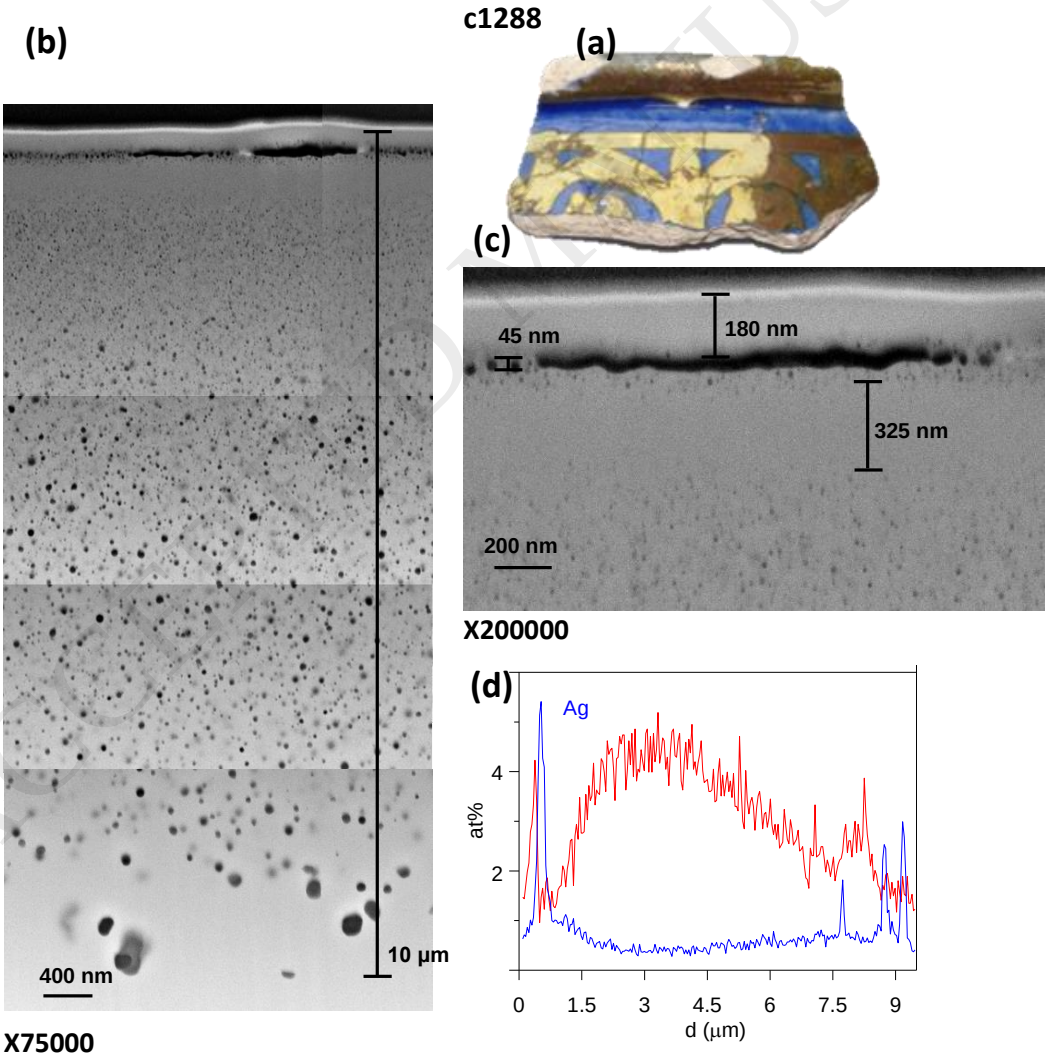

Figure 7. UV-Vis spectra (Left) and μ-XRD patterns, corresponding to (a) *Tell Minis* (EA2217r), (b) *Raqqa* (p620r) and (c) *Damascus II* (c1295) lustre layers.

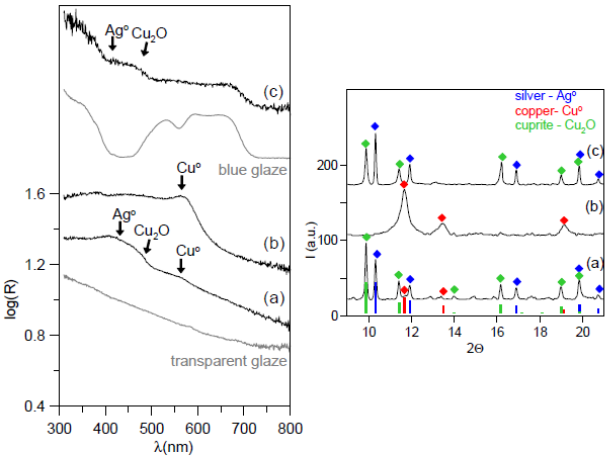

Figure 8. XANES data from a selection of lustres from *Tell Minis, Raqqa and Damascus* (solid lines) along with the least squares fit (dashed lines) to model compound data. The model compound data used from copper metal, Cu_2O and CuO are also shown. A selection of characteristic features are highlighted and discussed in the text.

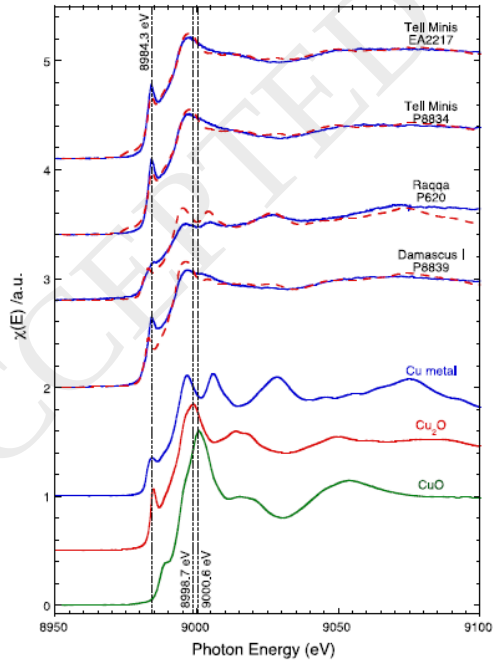

Figure 9. EXAFS R-space data, showing the distance of neighbouring atomic shells from a central copper atom, from one *Raqqa* and two *Damascus* samples (solid lines) along with the model fits (dashed lines). Comparisons with model compound data of copper metal, Cu_2O and CuO are also shown.

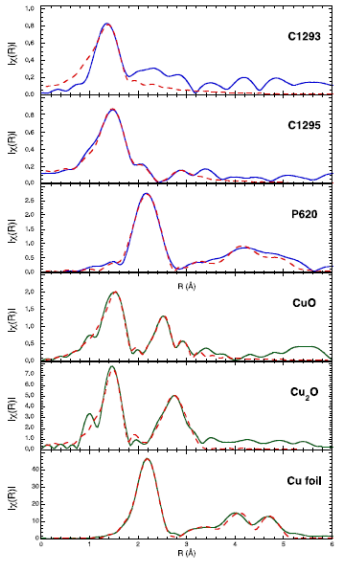

Figure 10. *Lightness L**, *chroma c** and *hue h** determined using the protocol accepted by the International Commission for Illumination CIE L*a*b*. From the total reflected light calculated from a continuous nanometric silver metallic layer over a glass substrate using Fresnel equations (transfer matrix method) as a function of the thickness of the layer.

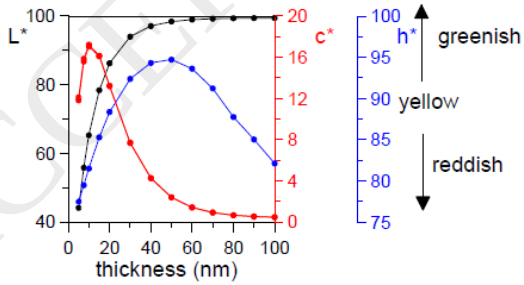

Table I. SEM-EDS analyses of the glazes.

		Na_2O	K_2O	Al_2O_3	SiO_2	CaO	MgO	FeO	CoO	CuO	ZnO	SnO_2	PbO
Tell Minis	EA2217r	13.6 (0.4)	1.9 (0.1)	1.7 (0.1)	57.7 (1.0)	4.9 (0.4)	2.7 (0.2)	0.3 (0.3)					17.2 (0.6)
	p8834/36	10.9 (0.9)	1.6 (0.2)	1.3 (0.3)	64.1 (3.8)	3.7 (0.3)	1.6 (0.1)	0.7 (0.1)		0.3 (0.1)		0.3 (0.2)	15.0 (2.7)
Raqqa	p9404f	15.9 (0.2)	2.1 (0.1)	1.6 (0.1)	70.6 (0.4)	5.0 (0.1)	3.3 (0.2)	0.9 (0.1)					
	p9404r	10.6 (2.1)	1.9 (0.2)	1.4 (0.2)	78.9 (3.7)	3.5 (0.8)	1.8 (0.3)	0.8 (0.1)					
	p620r	7.6 (0.7)	1.9 (0.4)	1.3 (0.2)	78.6 (2.0)	6.6 (2.0)	2.2 (0.3)	1.0 (0.2)					
	p620f	11.6	1.7	1.2	73.0	7.2	2.9	0.9					
	p9403f	11.8 (3.7)	1.9 (0.2)	1.6 (0.3)	76.5 (5.9)	4.6 (1.7)	2.0 (0.5)	0.8 (0.1)					
	p18777f	9.0 (0.9)	1.7 (0.2)	1.7 (0.3)	79.1 (2.4)	4.1 (0.6)	1.7 (0.2)	0.9 (0.1)					
	p18779f	11.3 (4.3)	2.2 (0.3)	1.5 (0.2)	76.5 (6.4)	4.1 (1.0)	2.4 (0.3)	0.9 (0.5)					
	p18779r	14.2 (1.0)	2.3 (0.1)	1.4 (0.2)	72.2 (2.0)	4.9 (0.5)	2.5 (0.1)	0.7 (0.1)					
Damascus I	p8839	10.0 (0.1)	1.5 (0.01)	2.0 (0.0)	46.5 (0.0)	5.2 (0.1)	2.2 (0.03)	1.3 (0.1)	0.5 (0.1)			4.9 (0.2)	25.6 (0.2)
	c1293r	8.7 (0.2)	1.2 (0.04)	0.8 (0.1)	61.0 (0.6)	2.3 (0.1)	1.3 (0.06)	0.4 (0.1)	0.2 (0.04)	0.3 (0.1)			22.9 (0.3)
	c1293f	8.4 (0.2)	1.3 (0.1)	1.2 (0.3)	59.9 (0.4)	2.6 (0.1)	1.4 (0.2)	3.1 (0.04)	0.7 (0.2)	1.0 (0.1)	1.2 (0.3)		19.4 (0.1)
Damascus II	c1295	11.7 (0.2)	4.1 (0.1)	0.9 (0.0)	70.3 (0.5)	6.1 (0.1)	4.4 (0.2)	1.4 (0.1)	0.3 (0.1)				
	c1288	11.2 (0.2)	3.4 (0.05)	1.2 (0.1)	69.6 (0.3)	8.0 (0.5)	4.3 (0.2)	1.3 (0.1)	0.1 (0.1)				

Table II. Summary of the lustre layers composition and microstructure. Data obtained from RBS for those layers thinner than 2 µm[a] and FIB analysis for thicker layers[b]. Size of the nanoparticles obtained from SEM-FIB images[c], spherical particles are observed for the *Tell Minis* and *Raqqa* lustre while the particles coalescence near the surface into a continuous nano-layer is observed in the *Damascus*. Copper chemical species determined from Xanes fitted data[d] and from EXAFS fitted data[e].

	sample	layer composition			Cu peak		Ag peak		copper[c]	silver[c]	layer	Copper species	
		mean Cu	mean Ag	%Cu (Cu+Ag)	Max.	position	Max.	position	particles	particles	thickness	(%)	
		(wt %)	(wt %)	(wt %)	(at %)	(µm)	(at %)	(µm)	(nm)	(nm)	(µm)	Cu^o	Cu_2O
Tell Minis[a]	EA2217	6.5	3.0	68	4.1	0.8	2.1	<0.2	Cuprite/ some Cu^o ~50	Ag^o <20	1.5	22[d]	78[d]
	p8834/36	5.4	2.4	70	7.0	1.2	6.4	0.1			2.1	22[d]	78[d]
Raqqa[a]	p9404r	13.8	2.1	87	8.0	0.1	1.0	0.2	Cu^o <20	Ag^o -	0.5		
	P620f	8.3	0.1	99	12.2	0.2	0.2	0.2			0.4	64[d]	36[d]
	P620r	13.8	0.3	98	12.8	0.2	0.2	0.2			0.5	100[e]	
	p9403	11.4	0.2	98	9.5	0.2	0.2	0.2			0.4		
	p18777f	6.7	0.1	98	7.5	0.2	0.1	0.1			0.4		
	p18777r	10.4	0.2	98	15.0	0.1	0.1	0.1			0.5		
	p18779r	3.8	0.1	99	6.5	0.1	0.1	0.2			0.5		
Damascus I[b]	p8839	3.5	1.2	75	4.0	0.2	3.0	0.2	Cuprite/ some Cu^o <80	Ag^o 40 x 100	5.2	30[d]	70[d]
	c1293	6.2	4.9	56	3.2	1.5	3.5	0.3	Cuprite <80	Ag^o 40 x 400	4.0		100[e]
Damascus II[b]	c1295f	5.5	3.8	59	2.5	2.5	1.5	0.2	Cuprite <80	Ag^o 40 x 1000	5.7		100[e]
	c1295r	7.4	3.6	67	3.0	2.8	1.0	0.3			5.6		100[e]
	c1288	8.3	2.3	78	4.5	2.8	5.5	0.2			8.8		